Bioorganic & Medicinal Chemistry 18 (2010) 978–983

Contents lists available at ScienceDirect

Bioorganic & Medicinal Chemistry

journal homepage: www.elsevier.com/locate/bmc

Cell permeability of Py–Im-polyamide-fluorescein conjugates: Influence of molecular size and Py/Im content

Shigeki Nishijima [a], Ken-ichi Shinohara [a], Toshikazu Bando [a,*], Masafumi Minoshima [a], Gengo Kashiwazaki [a], Hiroshi Sugiyama [a,b,*]

[a] Department of Chemistry, Graduate School of Science, Kyoto University, Sakyo, Kyoto 606-8501, Japan
[b] Institute for Integrated Cell-Material Sciences, Kyoto University, Sakyo, Kyoto 606-8502, Japan

ARTICLE INFO

Article history:
Received 10 June 2009
Revised 6 July 2009
Accepted 7 July 2009
Available online 16 July 2009

Keywords:
Polyamide
DNA binder
Flow cytometry
Cell permeability

ABSTRACT

In order to investigate the influence of molecular size and pyrrole (Py)/imidazole (Im) content on the cell permeability of Py–Im-polyamide-fluorescein conjugates we systematically designed the Py-polyamides and Im-polyamides. Flow cytometric analysis revealed that Py-polyamides, even those with large molecular size, **P-15** and **P-18**, showed good cellular uptake, but Im-polyamides showed very poor uptake. Fluorescence microscopy revealed that conjugate **P-6** exhibited nuclear localization, while **P-18** showed less nuclear stain but intracellular localization, suggesting that increased molecular size is one of the determinants in reducing nuclear access. Furthermore, results for hairpin polyamide conjugates **H-1**, **H-2**, and **H-3** containing different Py/Im content indicated that cellular uptake increases as the Im residue is reduced. It appears that Py–Im-polyamide has general properties regardless of whether they have a linear or a hairpin structure.

1. Introduction

Minor-groove-binding compounds that are composed of *N*-methylpyrrole (Py) and *N*-methylimidazole (Im) recognize each of the Watson–Crick base pairs. An antiparallel pairing of Im opposite Py (Im–Py pair) distinguishes a G–C from a C–G, whereas a Py–Py pair binds both A–T and T–A in preference to G–C/C–G base pairs.[1] A variety of sequence-specific Py–Im-polyamides to target sequences of biological interest have been developed[2] and have been widely studied for not only regulating gene expression but also bioimaging,[3] because polyamides cross the plasma membrane and the nuclear envelope to bind to the target chromosomal DNA. Recently, Dervan and coworkers demonstrated cellular and nuclear localization of polyamide-fluorophore conjugates by confocal laser scanning microscopy,[4] and also the polyamide concentration inside the cell nucleus by flow cytometry techniques.[5] Permeability of polyamides depends on a wide variety of molecular determinants such as Py/Im content, number and location of positive and negative charges, presence of a b-alanine residue at the C-terminus, choice of fluorophore, linker composition and attachment.[4c] Nonetheless it is a complicated task to predict a priori the subcellular distribution of a particular polyamide-fluorophore conjugate. Therefore, simple polyamides should be examined to understand the effect of each of the determinants. In this paper, in an effort to determine the influence of molecular size and Py/Im content on cellular uptake, polyamides (Py-polyamides and Im-polyamides) with systematically different molecular sizes were designed and investigated using flow cytometry. Fluorescent activated cell sorting (FACS) analysis revealed that Py-polyamides with large molecular size have good cellular uptake but low nuclear uptake, and Im-polyamides have low uptake, regardless of molecular size. It was also found that cellular uptake increases as the Im residue decreases, as observed in the case of hairpin polyamides, which suggests that polyamides exhibit these properties regardless of whether they have a linear or a hairpin structure.

2. Molecular design and synthesis

We synthesized the Py-polyamide-fluorescein conjugates (**P-3**, **P-6**, **P-9**, **P-12**, **P-15**, **P-18**), and Im-polyamide-fluorescein conjugates (**I-3**, **I-6**, **I-9**, **I-12**) as shown in Figure 1. Polyamide conjugates with (b-PyPyPy or b-ImImIm)$_n$ (n = 1–6) blocks were increased systematically. A b-alanine residue was incorporated in order to allow the polyamides to be flexible.[6] Precursors of polyamide conjugates, which have *N*,*N*-(dimethylamino)propylamine (Dp) at the C-terminals and *tert*-butoxycarbonyl (Boc) protecting groups at the N-terminals, were prepared by Fmoc solid-phase synthesis, using a Py-coupled oxime resin or Im-coupled CLEAR resin, followed by Dp treatment.[7] After deprotection of the Boc group with trifluoroacetic acid (TFA) the precursor was conjugated with fluorescein isothiocyanate (FITC) and diisopropylethylamine (DIEA) to afford the

* Corresponding authors. Tel.: +81 75 753 4002; fax: +81 75 753 3670 (H.S.).
E-mail address: hs@kuchem.kyoto-u.ac.jp (H. Sugiyama).

0968-0896/$ - see front matter © 2009 Elsevier Ltd. All rights reserved.
doi:10.1016/j.bmc.2009.07.018

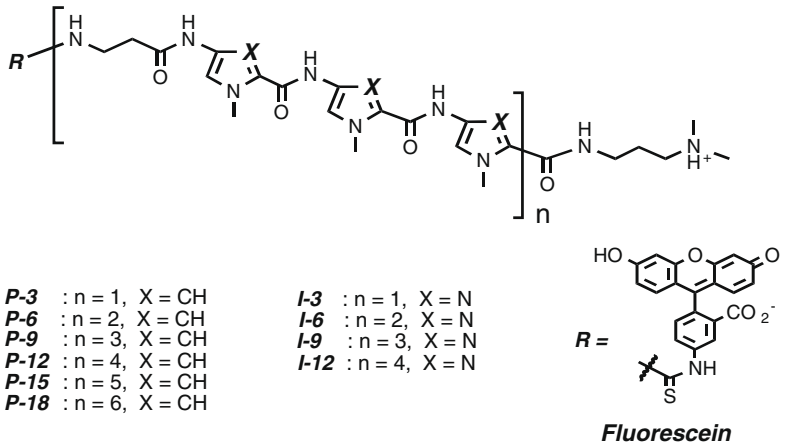

Figure 1. Chemical structures of Py-polyamide-fluorescein conjugates **P-3**, **P-6**, **P-9**, **P-12**, **P-15**, **P-18** and Im-polyamide-fluorescein conjugates **I-3**, **I-6**, **I-9**, **I-12**, which were synthesized in this work.

polyamide-fluorescein conjugates. Conjugates **P-15** and **P-18** were difficult to prepare by Fmoc solid-phase synthesis due to their reduced coupling efficiency. Therefore, we accomplish their synthesis by using a combination of solid- and liquid-phase synthesis. Conjugate **P-15**, as shown in scheme 1, was synthesized by the coupling of H_2N-(b-PyPyPy)$_2$Dp with Boc-(b-PyPyPy)$_3$-CO_2H, prepared by Fmoc solid-phase synthesis, and then purified, followed by conjugation of FITC. Conjugate **P-18** was prepared by the coupling of H_2N-(β-PyPyPy)$_2$Dp and Boc-(β-PyPyPy)$_4$-CO_2H, using a method similar to that described above. **P-18** is probably the largest polyamide ever prepared. The structures of Py-polyamides and Im-polyamides were identified by electrospray ionization time-of-flight mass spectrometry (ESI-TOFMS) after purification by reverse-phase HPLC.

3. Cellular uptake studies

To determine the influence of polyamide conjugates of different molecular sizes and Py/Im content, we investigated the cellular uptake of polyamide conjugates by flow cytometry. HEK293 cells have been widely used in cell biology research, especially for transfection. Cells were incubated with the polyamides for 24 h at 37 °C. After washing and then fixation with 3.7% formaldehyde in PBS, the fluorescence was measured by analyzing 10,000 cells by flow cytometry. Cell labeling was expressed using two parameters: the percentage of labeled cells and the relative median fluorescence (RMF). The latter was obtained by dividing the median fluorescence of labeled cells by the median fluorescence of unlabeled cells. Data from the resulting histogram (Fig. 2a) were plotted as the RMF and the percentage of labeled cells in Figure 2b. A high cellular uptake by the Py-polyamide conjugates, except **P-3**, was observed (labeled cells of **P-6**, **P-9**, **P-12**, **P-15**, **P-18**: >82%; **P-3**: 53%). The poor uptake of **P-3** was related to the fact that the tripyrrole like distamycin derivative is unable to induce intracellular cell fluorescence.[8] The RMF values of the conjugates **P-6**, **P-9**, **P-12**, **P-15** and **P-18** were 19.7, 24.5, 6.36, 17.7 and 18.2, respectively. In our experiments the RMF values of **P-6** and **P-9** were always higher than those of **P-15** and **P-18**, indicating that the six- to nine-ring polyamides might be optimal for cellular uptake. However, it is interesting to note that even polyamides **P-15** and **P-18** of much larger molecular size showed comparable uptake to polyamides **P-6** and **P-9**. These results demonstrated that in this case molecular size does not play a role in cellular uptake. It appears that the smaller polyamides are generally more cell permeable because of their size and molecular weight. Their molecular weight is close to the average molecular weight of clinically useful drugs.[9] However, we report that large polyamides could be permeable to cell membrane, suggesting excellent permeability of polyamides.

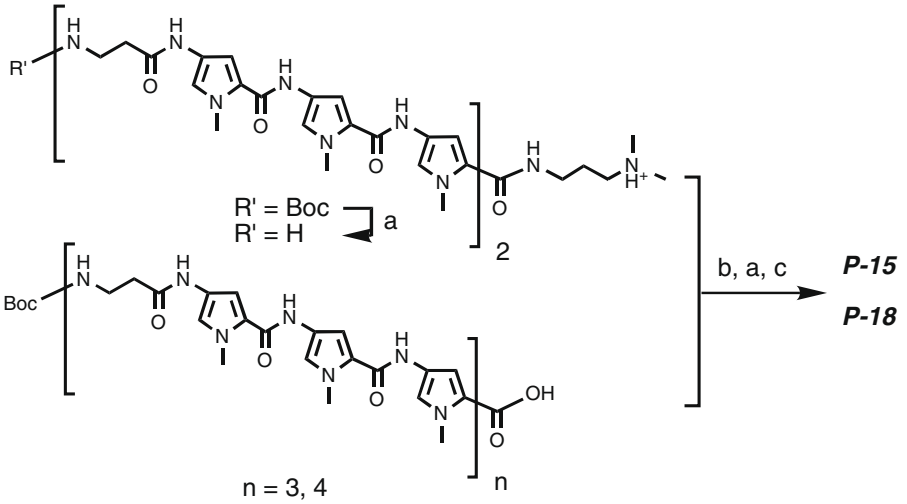

Scheme 1. Synthesis scheme for the preparation of conjugates P-1**5**, **P-18**. Reagents: (a) TFA/DCM (1:1 v/v) (b) PyBOP, DIEA, DMF (c) FITC, DIEA, DMF.

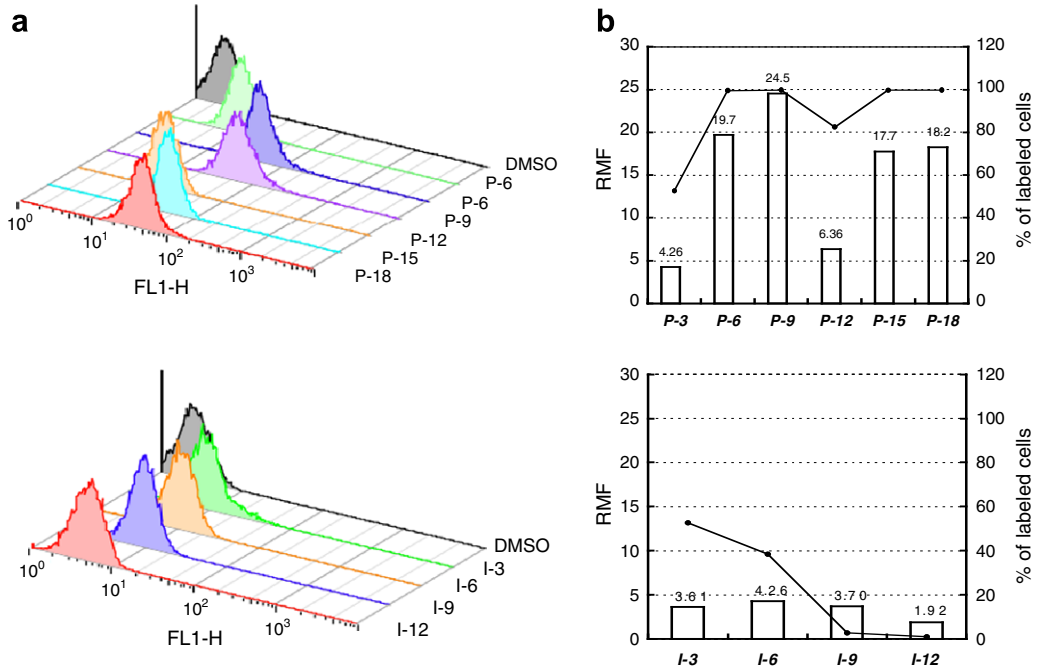

Figure 2. Cellular uptake analysis for polyamide-fluorescein conjugates by flow cytometry. (a) Histograms showing the cellular uptake for Py-polyamide (upper) and Im-polyamide (lower). HEK293 cells were incubated with 1 μM polyamides at 37 °C for 24 h. (b) Data from histograms were plotted as the relative median fluorescence (RMF) and percentage labeled cells (black bars: RMF, black lines: % of labeled cells).

In contrast, Im-polyamides showed very poor uptake (labeled cells of **I-3**: 53%, **I-6**: 39%, **I-9**: 3.0%, **I-12**: 1.1%). The RMF values of **I-6**, which was the highest value of the Im-polyamides, was 4.26 as low as that of **P-3**. In this case the cellular uptake decreased as the molecular size increased, clearly demonstrating that the Im unit is a negative determinant for cellular uptake. According to Dervan et al., replacement of Py with Im is nearly always a negative determinant for nuclear access, although there is no general correlation between the number of Im residues and uptake efficiency.[4c] Our results indicate that the reduced nuclear access they observed may be caused by the Im unit. A more detailed investigation of the correlation between Im-polyamide and cell permeability is ongoing.

We next examined the intracellular distribution of polyamide conjugates by fluorescence microscopy. Cells were incubated under the same as conditions as for flow cytometry. Cells with **P-6** showed fluorescence in the nucleus (Fig. 3), but cells with **I-6** did not show clear fluorescence which exceeded background fluorescence (data not shown). These results correspond with those of flow cytometry analyses. It should be noted however that cells with **P-18** showed fluorescence not only in the nucleus but also in the cytoplasm. In order to confirm nuclear access we proceeded to stain chromosomes using **P-18** and **P-6** (exposure time: **P-18** 7.0 s vs **P-6** 2.5 s). We observed clear differences between them (Fig. 4) despite the fact that the RMF values of **P-18** and **P-6** were similar in flow cytometry analyses. These results demonstrated that **P-18** was mainly in the cytoplasm, and not in the nucleus (**P-15** was mainly in the cytoplasm, but **P-9** was in the nucleus, data is not shown), suggesting that molecular size is a determinant for nuclear membrane permeability. Moreover, the bright dots in cytoplasm were observed for both polyamide conjugates **P-18** and **P-6,** especially **P-18** (Fig. 3). Although it is not sure that polyamide conjugates accumulate in a portion of the Golgi apparatus, lysosomes, or vesicles, it is presumably due to lipophilicity of polyamides, which may prevent polyamides going through nuclear membrane. Our study therefore strongly supports the fact that one of determinants for the reduction of nuclear access is increased molecular size.[4b]

Furthermore, to examine whether these results apply to hairpin polyamides **H-1**, **H-2**, **H-3** with different Py/Im content were synthesized, and evaluated by flow cytometry in MCF-7 cells (Fig. 5). **P-6** and **I-6** were selected due to their high and low cell permeabilities. MCF-7 cells were incubated with polyamides for 24 h at 37 °C. Because MCF-7 is more permissive cell type compared with HEK293,[4c] we also examined whether the cellular uptake by these polyamides depends on cell types or not. A significant increase in uptake was found for **P-6** (RMF: HEK293/MCF-7 = 19.7/210) but not for **I-6** (3.61/2.75). Regardless of cell type, Im-polyamides have very low permeability. Hairpin polyamide exhibited excellent cellular uptake (labeled cells: >90%). When we compared the RMF values of **P-6** with hairpin polyamides, surprisingly, **P-6** showed higher fluorescence than hairpin polyamides. It is unclear whether this is caused by the turn residue sequence (γ or β), one of the structural elements in the polyamide design.[4b] The RMF values of hairpin polyamides were as follows: **H-1 > H-2 > H-3**. These results can be explained by the Im effect, as described previously. Because **H-1** has no imidazole, **H-2** has two imidazoles and **H-3** has three imidazoles, the uptake of polyamide might increase as the Im content decreases. This suggests that the influence of the Py/Im content, observed in case of linear polyamides, also plays a role in the hairpin polyamides.

4. Conclusion

We studied the influence of molecular size and Py/Im content on the cellular uptake using flow cytometry. It was found that the molecular size of the Py-polyamides does not play a role in cellular uptake, although the nuclear membrane permeability is reduced. The Im-polyamides showed low uptake, and the uptake increased as the content of Im decreased in the case of hairpin polyamide, suggesting that the influence of Py/Im content, as observed in the case of linear polyamide, also pertains to hairpin polyamides. We anticipate that this greater understanding of cell permeability should prove useful for designing more efficient polyamides for targeting DNA in cancer cells.

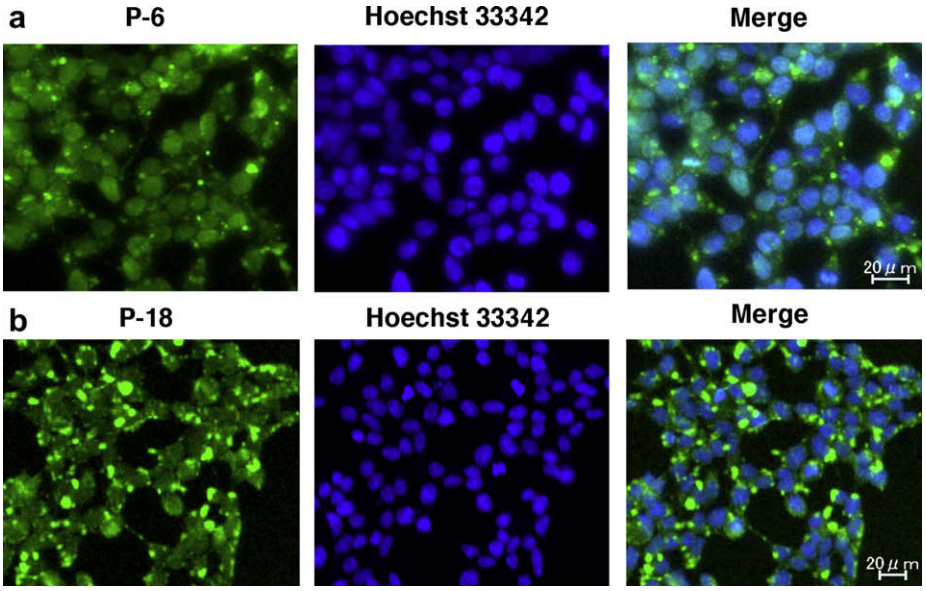

Figure 3. Cellular localization of polyamide conjugate **P-6**, **P-18** and nuclear stain Hoechst 33342 in adherent HEK293 cells. Cells were treated with 1 mM polyamide-fluorescein conjugates (24 h at 37 °C) and 20 mM Hoechst 33342 (1 h at 37 °C). (a) Fluorescence signals from **P-6** and Hoechst 33342 colocalize in cell nuclei. (b) **P-18** localize in cytoplasm entirely.

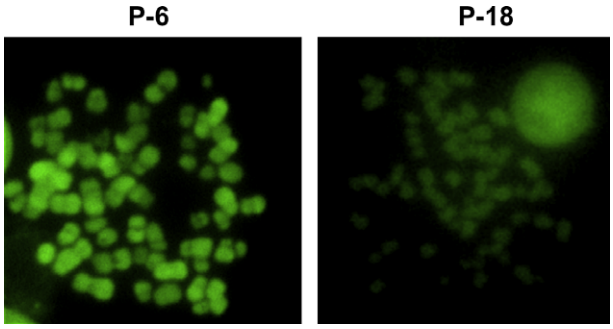

Figure 4. Chromosomes prepared from K562 cells were stained with **P-6** (left) and **P-18** (right). Colcemid treatment was performed 2 h before observation. Exposure time of **P-6** and **P-18** was 2.5 s and 7 s, respectively. Note that chromosomes with **P-6** appear bright green, but those with **P-18** do not.

5. Experimental

5.1. General methods

Reagents and solvents were purchased from standard suppliers and used without further purification. Abbreviations of some reagents: Fmoc, fluorenylmethoxy-carbonyl; Boc, *tert*-butoxycarbonyl; TFA, trifluoroacetic acid; DIEA, *N*,*N*-diisopropylethylamine; DMF, *N*,*N*-dimethyl-formamide; HCTU, 1-bis(dimethylamino)methylene]-5-chloro-1H-benzotriazolium 3-oxidehexafluorophosphate; PyBOP, benzotriazole-1-yl-oxy-trispyrrolidinophosphonium hexafluorophosphate; FITC, fluorescein isothiocyanate; DCM, dichloromethane. Oxime resin (200–400 mesh) and CLEAR-acid resin (100–200 mesh) were purchased from Novabiochem and PEPTIDES International, respectively. Electrospray ionization time-of-flight mass spectrometry (ESI-TOFMS) were produced on an API 150 (PE SCIEX) and BioTOF II (Bruker Daltonics) mass spectrometer. HPLC purification was performed with a Chemcobond 5-ODS-H reversed phase column (10 × 150 mm) in 0.1% AcOH with acetonitrile as eluent at a flow rate of 3.0 ml/min, appropriate gradient elution conditions, and detection at 254 nm.

5.2. Solid-phase synthesis of Py–Im-polyamide-fluorescein conjugates

5.2.1. FITC-(β-XXX)$_n$-Dp (X = Py or Im, n = 1–4) (P-3, P-6, P-9, P-12, and I-3, I-6, I-9, I-12)

Boc-(β-PyPyPy)$_n$-CO$_2$-oxime resin or Boc-(b-ImImIm)$_n$-CO$_2$-CLEAR resin were synthesized in a stepwise reaction by Fmoc solid-phase protocol. A sample of resin was cleaved with 2 mL of Dp at 55 °C overnight. The resin was removed by filtration, washed with DMF and methanol, concentrated in vacuo, and then triturated by diethyl ether. The crude polyamides were used in the next step without further purification. After deprotection of Boc with TFA, the crude polyamides were allowed to react at rt in DMF with FITC (1 equiv) and DIEA (20 equiv) to yield FITCpolyamide conjugates. After reaction at rt for 2 h, the resulting FITC polyamide conjugates were purified by HPLC using a Chemcobond 5-ODS-H column (0.1% AcOH/CH$_3$CN 0–100% linear gradient, 0–20 min, 254 nm).

5.2.2. FITC-(β-PyPyPy)5-Dp (P-15)

Both Boc-(β-PyPyPy)$_2$-Dp and Boc-(β-PyPyPy)$_3$-Dp were prepared by Fmoc solid-phase synthesis as described above. After treatment of Boc-(β-PyPyPy)$_3$-Dp with TFA, the crude polyamide was allowed to react at rt in DMF with PyBOP (1 equiv) and DIEA (20 equiv), then purified by HPLC. The resulting polyamide was allowed to deprotection and reacted at rt in DMF with FITC (1 equiv) and DIEA (20 equiv) to yield FITC-(β-PyPyPy)$_5$-Dp.

5.2.3. FITC-(β-PyPyPy)6-Dp (P-18)

A synthetic procedure similar to that used for preparation of compound **P-15**, using Boc-(β-PyPyPy)$_2$-Dp and Boc-(β-PyPyPy)$_4$-Dp, was followed to prepare FITC-(β-PyPyPy)$_6$-Dp.

The identity and purity of each compound was verified by analytical HPLC, UV–vis spectroscopy and electrospray ionization mass spectrometry (ESIMS) and electrospray ionization time-of-flight mass spectrometry (ESI-TOFMS).

FITC-(β-PyPyPy)-Dp. (**P-3**): ESI-TOFMS *m/z* calcd for $C_{47}H_{49}N_{10}O_9S$ $[M+H]^+$ 929.33, found 929.35.

FITC-(β-PyPyPy)$_2$-Dp. (**P-6**): ESI-TOFMS *m/z* calcd for $C_{68}H_{72}N_{17}O_{13}S$ $[M+H]^+$ 1366.51, found 1366.81.

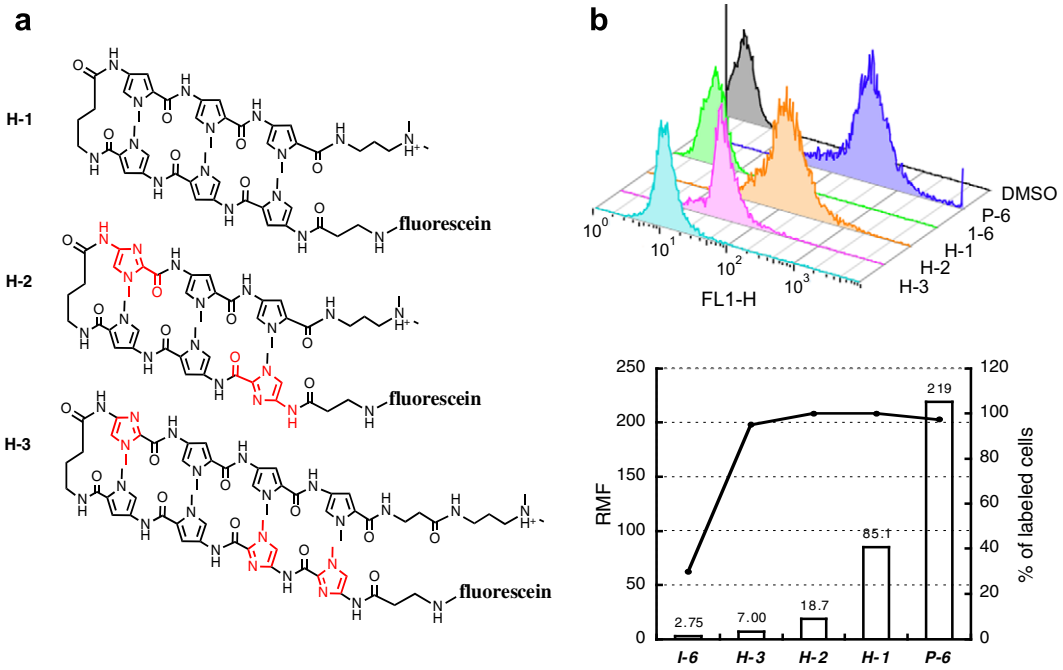

Figure 5. (a) Chemical structures of conjugates **H-1**, **H-2** and **H-3** (b) Flow cytometer experiments with MCF-7 cells incubated with 1 μM polyamide-fluorescein conjugates **P-6**, **I-6**, **H-1**, **H-2** and **H-3** under the same condition as HEK293. Data from histogram (upper) are plotted as percentage of labeled cells and RMF (lower).

FITC-(β-PyPyPy)$_3$-Dp. (**P-9**): ESI-TOFMS *m/z* calcd for $C_{89}H_{95}N_{24}O_{17}S$ $[M+H]^+$ 1803.69, found 1803.63.

FITC-(β-PyPyPy)$_4$-Dp. (**P-12**): ESI-TOFMS *m/z* calcd for $C_{110}H_{118}N_{31}O_{21}S$ $[M+H]^+$ 2240.88, found 2240.93.

FITC-(β-PyPyPy)$_5$-Dp. (**P-15**): ESI-TOFMS *m/z* calcd for $C_{131}H_{141}N_{38}O_{25}S$ $[M+2H]^{2+}$ 1339.53, found 1339.66.

FITC-(β-PyPyPy)$_6$-Dp. (**P-18**): ESI-TOFMS *m/z* calcd for $C_{152}H_{164}N_{45}O_{29}S$ $[M+2H]^{2+}$ 1558.12, found 1558.25.

FITC-(β-ImImIm)-Dp. (**I-3**): ESI-TOFMS *m/z* calcd for $C_{44}H_{46}N_{13}O_9S$ $[M+H]^+$ 932.32, found 932.36.

FITC-(β-ImImIm)$_2$-Dp. (**I-6**): ESI-TOFMS *m/z* calcd for $C_{62}H_{66}N_{23}O_{13}S$ $[M+H]^+$ 1372.49, found 1372.56.

FITC-(β-ImImIm)$_3$-Dp. (**I-9**): ESI-TOFMS *m/z* calcd for $C_{80}H_{86}N_{33}O_{17}S$ $[M+H]^+$ 1812.56, found 1812.93.

FITC-(β-ImImIm)$_4$-Dp. (**I-12**): ESI-TOFMS *m/z* calcd for $C_{98}H_{106}N_{43}O_{21}S$ $[M+H]^+$ 2252.82, found 2253.07.

5.5. Hairpin polyamide-fluorescein conjugates (H-1, H-2, H-3)

FITC polyamide conjugates were prepared using a synthetic procedure similar to that used for the preparation of FITC polyamide conjugates as previously described.

FITC-β-PyPyPy-γ-PyPyPy-Dp (**H-1**): ESI-TOFMS *m/z* calcd for $C_{69}H_{74}N_{17}O_{13}S$ $[M+H]^+$ 1380.53, found 1380.59.

FITC-β-ImPyPy-γ-ImPyPy-Dp (**H-2**): ESI-TOFMS *m/z* calcd for $C_{67}H_{72}N_{19}O_{13}S$ $[M+H]^+$ 1382.52, found 1382.57.

FITC-β-ImImPyPy-γ-ImPyPyPy-β-Dp (**H-3**): ESI-TOFMS *m/z* calcd for $C_{80}H_{88}N_{25}O_{15}S$ $[M+H]^+$ 1698.65, found 1698.80.

5.6. FACS analysis

Exponentially growing HEK293 cells or MCF-7 cells were trypsinized for 5 min at 37 °C, and seeded in fresh Dulbecco's Modified Eagle's Medium (DMEM) containing 10% fetal bovine serum (FBS), penicillin (100 units/mL) and streptomycin (100 μg/mL) solution to a concentration of 1.5×10^5 cells/mL in 12-well plates. Cells were grown in the culture plates for 72 h. The medium was then removed and replaced with 1 mL of fresh medium, followed by addition of 10 μL of the 100 μM polyamide solution for a final polyamide concentration of 1 μM. Cells were incubated in a 5% CO_2 atmosphere at 37 °C for 24 h. Following incubation, cells were washed with PBS, trypsinized for 5 min, neutralized the protease with RPMI 0.2% DMF solution, fixed in 3.7% formaldehyde in PBS, followed by acquisition with FACSCalibur and CELL Quest Pro Software (BD Bioscience). A total of 10,000 cells per sample were analyzed. The histogram analysis was performed using FlowJo.

5.7. Fluorescence microscopy

HEK 293 cells were maintained in DMEM containing 10% fetal bovine serum (FBS), penicillin (100 units/mL) and streptomycin (100 μg/mL) solution. Cell lines were trypsinized for 5 min at 37 °C, and resuspended in fresh medium to a concentration of 1.5×10^5 cells/mL. Cells were grown in the glass bottom dishes for 72 h. The medium was then removed and replaced with 1 mL of fresh medium, followed by addition of 10 μL of the 100 μM polyamide solution for a final polyamide concentration of 1 μM. After incubation in a 5% CO_2 atmosphere at 37 °C for 24 h, cells were washed two times with PBS to remove excess compound and they were analyzed. Hoechst 33342 (20 μM) was added to the medium before 1 h to observe by fluorescence microscopy. Imaging was performed with BZ-9000 (HS-all in one fluorescence microscopy, KEYENCE). FITC, Hoechst were excited using 480/40 nm, 360/40 nm laser lines. The emission signals were sorted out using a BZ510-filter, BZ460-50 filter, respectively. Exposure time for fluorescence was adjusted at each time point to localize fluorochromes. Image analysis was done using BZ analyzer Software.

5.8. Chromosome staining

K562 cells were maintained in RPMI-1640 containing 10% fetal bovine serum (FBS), penicillin (100 units/mL) and streptomycin (100 μg/mL) solution. K562 cells (8.5×10^5 cells/mL) were grown on plates with 10 μL of the 100 μM polyamide solution for a final

polyamide concentration of 1 μM, then incubated in a 5% CO_2 atmosphere at 37 °C for 24 h. Before pre-fixation, K562 cells were blocked mitotically by adding 10 μL of 10 μg/mL colcemid for 2 h. K562 cells were collected to tube and centrifuged at 500*g* for 10 min. After removing supernatant solution, the cells were swollen by treatment with a hypotonic buffer (60 mM KCl) for 30 min at 37 °C. The cells were fixed with a freshly methanol/acetic acid (3:1) solution for 10 min at room temperature, centrifuged 500*g* for 10 min, removing supernatant solution. This was carried out three times, then place a drop at the tilled slide, washed with methanol fixation and air dried overnight. Imaging was performed with a 100× oil-immersion objective lens on.

Acknowledgments

This work was supported by a Grant-in-Aid of Priority Research from the Ministry of Education, Culture, Sports, Science, and Technology, Japan, Academia Showcase for Japan Chemical Innovation Institute and JST, CREST. We thank Dr. Norio Nakatsuji (Institute for Integrated Cell-Material Sciences, Kyoto University) and Dr. Kaori Yamauchi (Stem Cell Research Center, Institute for Frontier Medical Sciences, Kyoto University) for performing flow cytometry analyses.

References and notes

1. For recent review, see: (a) Dervan, P. B. *Bioorg. Med. Chem.* **2001**, *9*, 2215–2235; (b) Dervan, P. B.; Edelson, B. S. *Curr. Biol. Curr. Opin. Str. Biol.* **2003**, *13*, 284–299.
2. (a) Wurtz, N. R.; Dervan, P. B. *Chem. Biol.* **2000**, *7*, 153; (b) Kwonj, Y.; Arndt, H. D.; Qian, M.; Choi, Y.; Kawazoe, Y.; Dervan, P. B.; Uesugi, M. *J. Am. Chem. Soc.* **2004**, *126*, 15940; (c) Bando, T.; Sugiyama, H. *Acc. Chem. Res.* **2006**, *39*, 935–944.
3. (a) Maeshima, K.; Janssen, S.; Laemmli, U. K. *EMBO J.* **2001**, *20*, 3218–3228; (b) Melanie, P. G.; Mark, D. F.; Heather, C. M.; Kevin, P. L.; Christine, O. D.; Peiwen, Z.; Cynthia, F.; van den Engh, G.; Mark, L. S.; Barbara, J. T. *Nucleic Acids Res.* **2002**, *30*, 2790–2799; (c) Fujimoto, J.; Bando, T.; Minoshima, M.; Kashiwazaki, G.; Nishijima, S.; Shinohara, K.; Sugiyama, H. *Bioorg. Med. Chem.* **2008**, *16*, 9741–9744; (d) Fujimoto, J.; Bando, T.; Minoshima, M.; Uchida, S.; Iwasaki, M.; Shinohara, K.; Sugiyama, H. *Bioorg. Med. Chem.* **2008**, *16*, 5899–5907.
4. (a) Belitsky, J. M.; Leslie, S. J.; Arora, P. S.; Beerman, T. A.; Dervan, P. B. *Bioorg. Med. Chem.* **2002**, *10*, 3313–3318; (b) Best, T. P.; Edelson, B. S.; Nickols, N. G.; Dervan, P. B. *Proc. Natl. Acad. Sci. U.S.A.* **2003**, *100*, 12063–12068; (c) Edelson, B. S.; Best, T. P.; Olenyuk, B.; Nickols, N. G.; Doss, R. M.; Foister, S.; Heckel, A.; Dervan, P. B. *Nucleic Acids Res.* **2004**, *32*, 2802–2818.
5. Hsu, C. F.; Dervan, P. B. *Bioorg. Med. Chem.* **2008**, *18*, 5851–5855.
6. Trauger, J. W.; Baird, E. E.; Mrksich, M.; Dervan, P. B. *J. Am. Chem. Soc.* **1996**, *118*, 6160–6166.
7. (a) Baird, E. E.; Dervan, P. B. *J. Am. Chem. Soc.* **1996**, *118*, 6141–6146; (b) Wurtz, N. R.; Turner, J. M.; Baird, E. E.; Dervan, P. B. *Org. Lett.* **2001**, *2*, 1201–1203; (c) Belitsky, J. M.; Nguyen, D. H.; Wurtz, N. R.; Dervan, P. B. *Bioorg. Med. Chem.* **2002**, *10*, 2767–2774.
8. Vazuez, O.; Blanco-Canosa, J. B.; Vazquez, M. E.; Martine-Costas, J.; Castedo, L.; Mascarenas, J. L. *ChemBioChem* **2008**, *9*, 1–9.
9. Yuan-Ping, P. *Bioorg. Med. Chem.* **2004**, *12*, 3063.